

## Synthesis of Colloidal Upconverting NaYF<sub>4</sub> Nanocrystals Doped with Er<sup>3+</sup>, Yb<sup>3+</sup> and Tm<sup>3+</sup>, Yb<sup>3+</sup> via Thermal Decomposition of Lanthanide Trifluoroacetate Precursors

John-Christopher Boyer,<sup>†</sup> Fiorenzo Vetrone,<sup>‡</sup> Louis A. Cuccia,<sup>†</sup> and John A. Capobianco<sup>\*†</sup>

*Department of Chemistry and Biochemistry, Concordia University, 7141 Sherbrooke Street West, Montreal, QC H4B 1R6, Canada, and Institut National de la Recherche Scientifique—Énergie, Matériaux et Télécommunications, Université du Québec, Varennes, QC J3X 1S2, Canada*

Received March 17, 2006; E-mail: capo@vax2.concordia.ca

The synthesis and spectroscopy of upconverting nanocrystals (NCs) have recently garnered considerable attention due to their potential use as biolabels and in biological assays.<sup>1–5</sup> Upconverting phosphors have a number of properties that make them attractive for use in these tasks.<sup>6–11</sup> Upconversion is the generation of higher energy light from lower energy radiation, usually near-infrared (NIR) or infrared (IR), through the use of transition metal, lanthanide, or actinide ions doped into a solid-state host. Organic dyes and semiconductor quantum dots that emit at higher energies via two-photon absorption processes requiring expensive high energy pulse lasers have also been investigated for use in these techniques.<sup>12–14</sup> Due to the relative high efficiency of the upconversion process in lanthanide-doped materials, inexpensive 980 nm NIR diode lasers may be employed as the excitation source. The realization of efficient NIR to visible upconverting NCs should unlock a realm of new possibilities in the field of biolabeling and bioassays.

The first step in achieving viable upconverting NCs is the selection of a material that is an efficient host for lanthanide ion upconversion. Gudel et al. have recently identified micrometer-sized Er<sup>3+</sup>/Yb<sup>3+</sup> or Tm<sup>3+</sup>/Yb<sup>3+</sup> co-doped hexagonal NaYF<sub>4</sub> as the material with the highest upconversion efficiencies.<sup>15–17</sup> Several recent publications have reported upconversion from colloids of either cubic<sup>1,5</sup> or hexagonal<sup>2</sup> NaYF<sub>4</sub> NCs, as well as hexagonal<sup>4,5</sup> NaGdF<sub>4</sub> NCs. It is well-known that metal trifluoroacetates thermally decompose to give the corresponding metal fluorides and various fluorinated and oxyfluorinated carbon species.<sup>18,19</sup> The use of oleic acid together with the noncoordinating solvent octadecene for the synthesis of various types of NCs is also well documented.<sup>20–22</sup> Here we present a new synthetic route for cubic NaYF<sub>4</sub> NCs that exploits the combination of these two facts to provide highly luminescent nanoparticles through a simple one-pot technique with only one preparatory step.

The procedure for the synthesis of NaYF<sub>4</sub> NCs was adapted from a recently reported synthesis of LaF<sub>3</sub> nanoplates.<sup>22</sup> The lanthanide trifluoroacetate precursors were prepared from the corresponding lanthanide oxides and trifluoroacetic acid.<sup>18</sup> The corresponding amount of sodium trifluoroacetate was then added to the reaction vessel with octadecene and oleic acid. The resulting solution was heated to 100 °C under vacuum with stirring for 30 min to remove residual water and oxygen. The solution was then heated to 300 °C at a rate of 10 °C/min under Ar and kept at this temperature for 1 h. Subsequently, the mixture was allowed to cool to room temperature, and the NCs were precipitated by the addition of hexane/acetone (1:4 v/v) and isolated via centrifugation. The resulting pellet was then washed once with ethanol and further purified by dispersing in a minimum amount of chloroform and precipitated with excess ethanol. The resulting NCs were dried

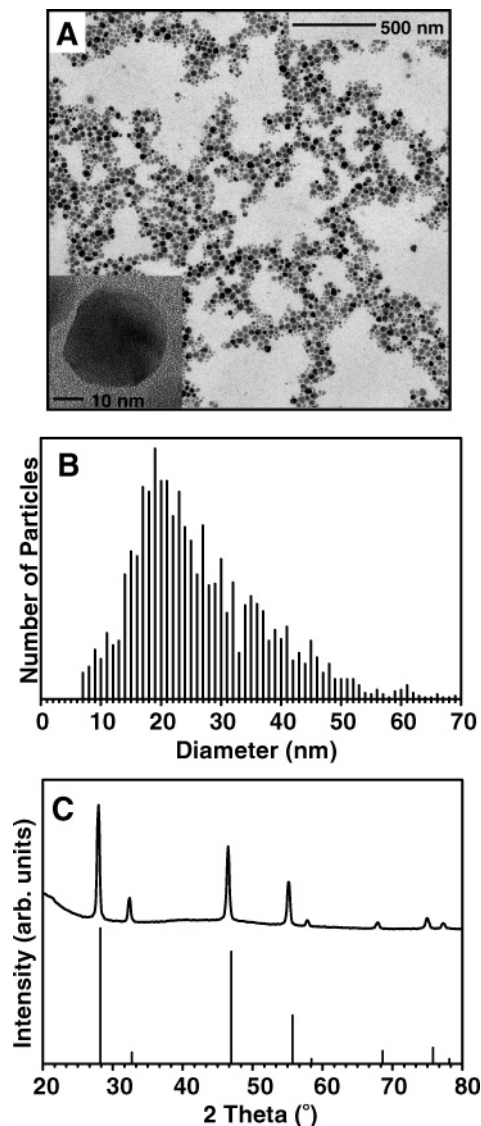
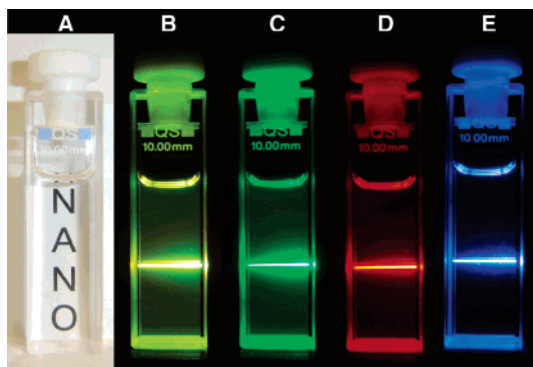


**Figure 1.** Characterization data for NaYF<sub>4</sub>: 2% Er<sup>3+</sup>, 20% Yb<sup>3+</sup> nanocrystals. (A) Transmission electron microscopy (TEM) image. Inset: High-resolution TEM (HRTEM) image of a single nanocrystal. (B) Histogram of the particle sizes obtained from TEM images of ~1400 nanocrystals. (C) Experimental powder X-ray diffraction (XRD) pattern (top curve) and the calculated line pattern for  $\alpha$ -NaYF<sub>4</sub> (bottom curve).

under vacuum for 24 h. The presence of the oleic acid ligand on the surface of the NCs was confirmed via the <sup>1</sup>H NMR of an undoped NaYF<sub>4</sub> sample (Figure S1 in Supporting Information). Due to the presence of the capping ligand, the NCs could be dispersed in nonpolar solvents and were colloiddally stable in solution for a period of weeks with no visible agglomeration or settling.

<sup>†</sup> Concordia University.

<sup>‡</sup> Université du Québec.



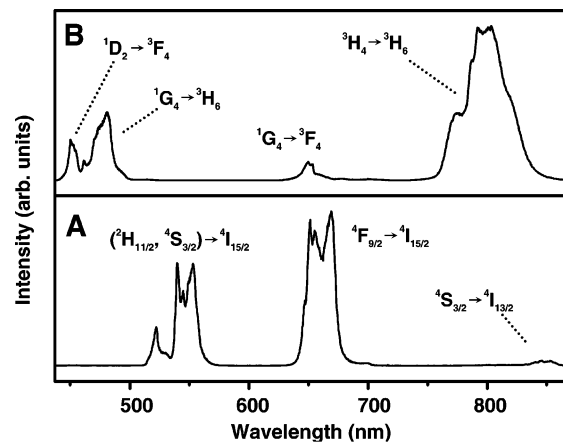
**Figure 2.** One wt % colloidal solutions of nanocrystals in dichloromethane excited at 977 nm demonstrating upconversion luminescence. (A) NaYF<sub>4</sub>: 2% Er<sup>3+</sup>, 20% Yb<sup>3+</sup> solution showing its transparency. (B) Total upconversion luminescence of NaYF<sub>4</sub>: 2% Er<sup>3+</sup>, 20% Yb<sup>3+</sup> solution. (C and D) NaYF<sub>4</sub>: 2% Er<sup>3+</sup>, 20% Yb<sup>3+</sup> upconversion viewed through green and red filters, respectively. (E) NaYF<sub>4</sub>: 2% Tm<sup>3+</sup>, 20% Yb<sup>3+</sup> solution.

Figure 1 shows the characterization data for a NaYF<sub>4</sub>: 2% Er<sup>3+</sup>, 20% Yb<sup>3+</sup> sample. The transmission electron microscopy (TEM) images (Figure 1A) show that the synthesized particles are roughly spherical. From the particle size distribution (Figure 1B), one can observe that the particles vary in size from 10 to 50 nm, with the majority falling in the range between 15 and 30 nm. The powder X-ray diffraction (XRD) pattern (Figure 1C) of the sample shows well-defined peaks, indicating the high crystallinity of the synthesized material. The peak positions and intensities from the experimental XRD pattern match closely with the calculated pattern for cubic  $\alpha$ -NaYF<sub>4</sub>.<sup>23</sup> From the line broadening of the diffraction peaks, the crystallite size of the sample was determined to be approximately 25 nm using the Debye–Scherrer formula, which corresponds well to the average particle size determined from the TEM data.

Figure 2A–D shows photographs of a 1 wt % solution of NaYF<sub>4</sub>: 2% Er<sup>3+</sup>, 20% Yb<sup>3+</sup> NCs in dichloromethane, demonstrating its transparency (Figure 2A) and the total visible upconversion luminescence under 977 nm excitation with a power density of 1.3 kW/cm<sup>2</sup> (Figure 2B). Figure 2C and D shows the same solution through appropriate green and red filters, respectively. Figure 2E demonstrates the upconversion luminescence of a 1 wt % solution of NaYF<sub>4</sub>: 2% Tm<sup>3+</sup>, 20% Yb<sup>3+</sup> in dichloromethane under the above excitation conditions.

The visible and NIR upconversion spectra of 1 wt % solutions of NaYF<sub>4</sub>: 2% Er<sup>3+</sup>, 20% Yb<sup>3+</sup> and NaYF<sub>4</sub>: 2% Tm<sup>3+</sup>, 20% Yb<sup>3+</sup> NCs in dichloromethane under 977 nm excitation are shown in Figure 3A and B, respectively. The spectra correspond to what has been reported previously for Er<sup>3+</sup> and Tm<sup>3+</sup> upconversion in cubic NaYF<sub>4</sub> NCs.<sup>1–5</sup> In the Er<sup>3+</sup> sample, green luminescence was observed from the (<sup>2</sup>H<sub>11/2</sub>, <sup>4</sup>S<sub>3/2</sub>) → <sup>4</sup>I<sub>15/2</sub> and red from the <sup>4</sup>F<sub>9/2</sub> → <sup>4</sup>I<sub>15/2</sub> transitions, respectively. The power dependencies of the green and red luminescence (Figure S2) were found to be approximately 2, indicating that two photons were involved in the upconversion mechanism. Four spectral bands were observed in the Tm<sup>3+</sup> sample and were assigned to the <sup>1</sup>G<sub>4</sub> → <sup>3</sup>H<sub>6</sub>, <sup>1</sup>D<sub>2</sub> → <sup>3</sup>F<sub>4</sub>, <sup>1</sup>G<sub>4</sub> → <sup>3</sup>F<sub>4</sub>, and <sup>3</sup>H<sub>4</sub> → <sup>3</sup>H<sub>6</sub> transitions. The mechanisms responsible for the upconversion luminescence are shown in the Supporting Information (Figure S3).

We have reported a novel and straightforward synthesis for upconverting lanthanide-doped NCs that requires few preparatory steps. The Er<sup>3+</sup>, Yb<sup>3+</sup> and Tm<sup>3+</sup>, Yb<sup>3+</sup> doped particles exhibit green/red and blue upconversion luminescence, respectively, under 977 nm laser excitation with low power densities. Further refinement of the synthesis is currently underway to obtain a narrower particle



**Figure 3.** Luminescence emission spectra of 1 wt % colloidal solutions of nanocrystals in dichloromethane excited at 977 nm. (A) NaYF<sub>4</sub>: 2% Er<sup>3+</sup>, 20% Yb<sup>3+</sup> and (B) NaYF<sub>4</sub>: 2% Tm<sup>3+</sup>, 20% Yb<sup>3+</sup>.

size distribution as well as core–shell NCs where a shell of undoped NaYF<sub>4</sub> is grown over the lanthanide-doped NaYF<sub>4</sub> core. Investigation of additional capping ligands and postsynthetic surface treatments are also ongoing to obtain water-dispersible NCs.

**Acknowledgment.** The authors gratefully acknowledge NSERC Canada for financial support.

**Supporting Information Available:** Full synthetic procedure, NMR of NaYF<sub>4</sub> sample, power dependence of upconversion emission, and upconversion mechanism diagrams. This material is available free of charge via the Internet at <http://pubs.acs.org>.

## References

- Heer, S.; Kömpe, K.; Güdel, H. U.; Haase, M. *Adv. Mater.* **2004**, *16*, 2102–2105.
- Zeng, J.-H.; Su, J.; Li, Z.-H.; Yan, R.-X.; Li, Y.-D. *Adv. Mater.* **2005**, *17*, 2119–2123.
- Wang, L.; Yan, R.; Huo, Z.; Wang, L.; Zeng, J.; Bao, J.; Wang, X.; Peng, Q.; Li, Y. *Angew. Chem., Int. Ed.* **2005**, *44*, 6054–6057.
- Aebischer, A.; Heer, S.; Biner, D.; Krämer, K.; Haase, M.; Güdel, H. U. *Chem. Phys. Lett.* **2005**, *407*, 124–128.
- Suyver, J. F.; Aebischer, A.; Biner, D.; Gerner, P.; Grimm, J.; Heer, S.; Krämer, K. W.; Reinhard, C.; Güdel, H. U. *Opt. Mater.* **2005**, *27*, 1111–1130.
- Kuningas, K.; Rantanen, T.; Ukonaho, T.; Lövgren, T.; Soukka, T. *Anal. Chem.* **2005**, *77*, 7348–7355.
- Corstjens, P. L. A. M.; Li, S.; Zuiderwijk, M.; Kardos, K.; Abrams, W. R.; Niedbala, R. S.; Tanke, H. J. *IEEE Proc. Nanobiotechnol.* **2005**, *152*, 64–72.
- Hirai, T.; Orikoshi, T. *J. Colloid Interface Sci.* **2004**, *273*, 470–477.
- Rijke, F. v. d.; Zijlman, H.; Li, S.; Vail, T.; Raap, A. K.; Niedbala, R. S.; Tanke, H. J. *Nat. Biotechnol.* **2001**, *19*, 273–276.
- Hampel, J.; Hall, M.; Mufti, N. A.; Yao, Y.-M. M.; MacQueen, D. B.; Wright, W. H.; Cooper, D. E. *Anal. Biochem.* **2001**, *288*, 176–187.
- Zijlman, H. J. M. A. A.; Bonnet, J.; Burton, J.; Kardos, K.; Vail, T.; Niedbala, R. S.; Tanke, H. J. *Anal. Biochem.* **1999**, *267*, 30–36.
- Denk, W.; Strickler, J. H.; Webb, W. W. *Science* **1990**, *248*, 73–76.
- König, K. *J. Microsc.* **2000**, *200*, 83–104.
- Larson, D. R.; Zipfel, W. R.; Williams, R. M.; Clark, S. W.; Bruchez, M. P.; Wise, F. W.; Webb, W. W. *Science* **2003**, *300*, 1434–1437.
- Krämer, K. W.; Biner, D.; Frei, G.; Güdel, H. U.; Hehlen, M. P.; Lüthi, S. R. *Chem. Mater.* **2004**, *16*, 1244–1251.
- Suyver, J. F.; Grimm, J.; Veen, M. K. v.; Biner, D.; Krämer, K. W.; Güdel, H. U. *J. Lumin.* **2006**, *117*, 1–12.
- Suyver, J. F.; Grimm, J.; Krämer, K. W.; Güdel, H. U. *J. Lumin.* **2005**, *114*, 53–59.
- Rüssel, C. *J. Non-Cryst. Solids* **1993**, *152*, 161–166.
- Rillings, K. W.; Roberts, J. E. *Thermochim. Acta* **1974**, *10*, 285–298.
- Yu, W. W.; Peng, X. *Angew. Chem., Int. Ed.* **2002**, *41*, 2368–2371.
- Park, J.; An, K.; Hwang, Y.; Park, J.-G.; Noh, H.-J.; Kim, J.-Y.; Park, J.-H.; Hwang, N.-M.; Hyeon, T. *Nat. Mater.* **2004**, *3*, 891–895.
- Zhang, Y.-W.; Sun, X.; Si, R.; You, L.-P.; Yan, C.-H. *J. Am. Chem. Soc.* **2005**, *127*, 3260–3261.
- Roy, D. M.; Roy, R. *J. Electrochem. Soc.* **1964**, *111*, 421–429.

JA061848B